

## Contribution to resilient and permanent deformation investigation of unbound granular materials with different geological origins from Rio Grande do Sul, Brazil

Amanda Vielmo Sagrilo<sup>1#</sup> , Paula Taiane Pascoal<sup>1</sup> , Magnos Baroni<sup>1</sup> ,

Ana Helena Back<sup>2</sup> , Rinaldo José Barbosa Pinheiro<sup>1</sup> , Luciano Pivoto Specht<sup>1</sup> ,

Antônio Carlos Rodrigues Guimarães<sup>3</sup> 

Article

### Keywords

Deformability  
Pavement  
Shakedown theory  
Granular base course  
Lithological origins

### Abstract

This article evaluates the resilient modulus and permanent deformation of granular materials of different lithological origins widely used as a pavements base layer in south Brazil. For this, a single particle size distribution was determined for the materials that were subjected to physical, chemical, mechanical characterizations, especially resilient modulus and permanent deformation by repeated load triaxial tests. It was noticed that the denser materials had a higher resilient modulus generated by increase in the sample's stiffness. For permanent deformation this tendency has not been maintained for all materials. Therefore, the granulation and structure of the materials can influence long-term tests. The Guimarães' model has proven to be adequate for the sample evaluation. For the shakedown research, samples showed accommodation and creep shakedown. The samples that presented accommodation had an increase in the resilient modulus after permanent deformation, while those that presented creep increased or decreased resilient modulus according to the material origin.

## 1. Introduction

Granular materials, used as a base layer for flexible pavements, influence the structure performance as a whole. In this layer, when the material receives and supports the stresses of traffic, successively returning to its original state throughout its service life, it is said that this material has a high resilient modulus (RM), preventing the formation of fatigue cracks on the pavement surface. Concomitantly, part of the deformations caused by traffic action are accumulated, called permanent deformations (PD) which, added to the deformations of other layers, are manifested on the pavement surface as rutting (Huang, 2004; Cerni et al., 2012; Erlingsson et al., 2017).

Shakedown theory is used to characterize soils and unbound granular materials employed in pavements (Werkmeister et al., 2001; Werkmeister, 2003; Werkmeister, 2006; Wang & Yu, 2013; Gu et al., 2017; Alnedawi et al., 2019a; Nazzal et al., 2020). According to the theory, the unbound

granular materials (UGM) can present three different ranges: range A or plastic shakedown, after a finite number of cycles, the accumulation of permanent deformations reaches a constant; range B or creep shakedown, the permanent strain rate decreases after a number of cycles, but the resilient strains are not constant and the stiffness decrease; range C or incremental collapse, the permanent deformation increases with the cycles. The UGMs can fail by shear or overstressing.

The main parameters that affect the elastic and plastic deformability of granular layers are the active stresses, the reorientation of the main stresses, the history of stresses, number, duration and frequency of loads, degree of compaction, moisture content, particle size distribution, maximum size of aggregates, fines content, type of aggregate and particle shape (Collins & Boulbibane, 2000; Lekarp et al., 2000; Lekarp & Isacsson, 2001; Song & Ooi, 2010; Xiao et al., 2019; Soliman & Shalaby, 2015). Among these factors, for the present study, the lithological origin of the aggregates that compound the granular material is emphasized.

<sup>#</sup>Corresponding author. E-mail address: amandavs94@gmail.com

<sup>1</sup>Universidade Federal de Santa Maria, Departamento de Transportes, Santa Maria, RS, Brasil.

<sup>2</sup>Faculdade Dom Alberto, Santa Cruz do Sul, RS, Brasil.

<sup>3</sup>Instituto Militar de Engenharia, Seção de Ensino de Engenharia de Fortificação e Construção, Rio de Janeiro, RJ, Brasil.

Submitted on September 22, 2022; Final Acceptance on May 18, 2023; Discussion open until November 30, 2023.

<https://doi.org/10.28927/SR.2023.009822>



This is an Open Access article distributed under the terms of the Creative Commons Attribution License, which permits unrestricted use, distribution, and reproduction in any medium, provided the original work is properly cited.

According to Xiao et al., (2019), Ba et al. (2015), Alnedawi et al. (2019b) and Alnedawi et al. (2021), granular materials composed of different lithological origins show different deformability behavior, even when the granulometric curve is similar among them. Lima et al. (2017) have analyzed two quarries of the same lithological origin and for the same granulometric curve obtained similar results in terms of resilience and permanent deformation. Nazzari et al. (2020) have conducted RM and PD tests of granular granite, sandstone and limestone materials. The mixtures' granulometric curves were similar, although the behavior in terms of resilience, permanent deformation and shakedown are considerably different.

In this paper, for the tests of the resilient modulus (DNIT, 2018a) and permanent deformation (DNIT, 2018b), repeated load triaxial (RLT) test has been used. Among the mathematical models employed for the RM behavior the following models stand out: model  $k-\sigma_3$ , dependent on the confining stress (Biarez, 1962), model  $k-\sigma_d$  as a function of the deviator stress (Svenson, 1980), model  $k-\theta$ , addressed by Seed et al. (1967), Compound model proposed by Pezo et al. (1992), and Universal model that had been presented by AASHTO (2004), in addition to the models by Witczak (Rada & Witczak, 1981) and Witczak & Uzan (1988). In the analysis of permanent deformation, the Guimarães' model (Guimarães, 2009; Guimarães et al., 2018), has been used, which proved to be adequate to the particularities of soils and tropical materials (Nogami & Villibor, 1991; Medina & Motta, 2015; Carvalho et al., 2015; Lima et al., 2020; Pascoal et al., 2021).

The objective of this study is to evaluate the resilient and permanent deformation behavior of three unbound granular materials from different lithological origins.

The characterization of the materials that compose the UGM and the results of tests and mathematical modeling of RM and PD and shakedown research are presented. The relevance of this study is related to the extensive use of granular bases regionally, due the abundance and variability of rock masses in the territory of the state of Rio Grande do Sul. Therefore, these materials should be characterized in terms of deformability. Besides, this study contributes to the database of the Brazilian M-E Design Method (MeDiNa), which is being implemented.

## 2. Materials and methods

### 2.1 Materials

To evaluate the influence of the lithological origin on the resilient behavior, permanent deformation and shakedown of the base course layer, three different types of mineral aggregates were selected. It is noteworthy that such materials came from different geomorphological provinces, including practically all lithological formations in the state of Rio Grande do Sul, Brazil. For this purpose, São Juvenal quarry and Della Pasqua quarry, named respectively as SJ and DPA, are originated from the Planalto Meridional Province, the geographical coordinates (UTM; Universal Transverse Mercator coordinate system) of which are, respectively: 22J – 251945.40 m W 6826112.10 m S and 22J – 228402.58 m W 6724545.40 m S. In contrast, the third material, originated from SBS Engenharia quarry, called SBS, is located in the Escudo Sul-Rio-Grandense Province under coordinates 22J – 357488.45 m W 6483361.81 m S. Figure 1 shows the unbound granular material analyzed in this study.

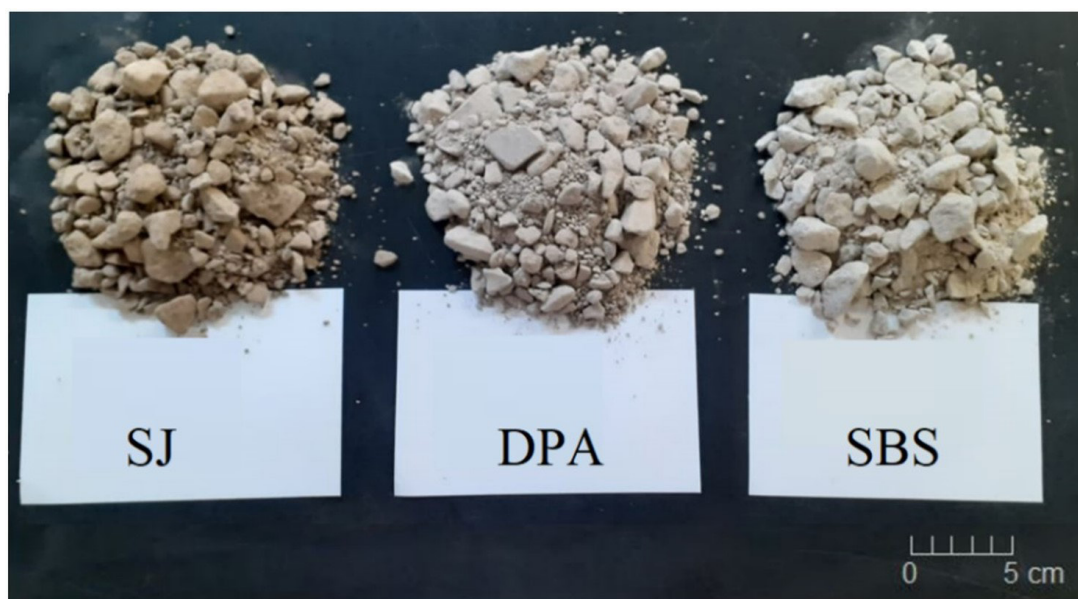


**Figure 1.** General aspect of the unbound granular material from different lithologies analyzed in this work.

The petrographic thin section slides provided the microscopic description of the textural, structural and mineralogical characteristics of the rocks, in addition to the physical and mechanical characterization tests. Table 1 presents the mineralogical composition, rock description and the physical and mechanical indexes.

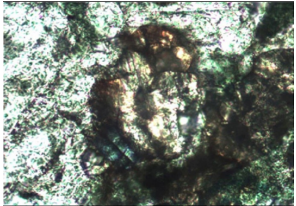
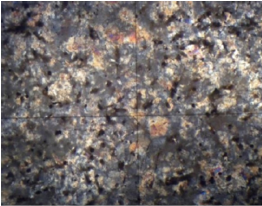
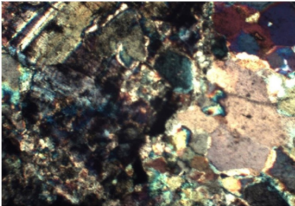
Based on Table 1, aggregates mechanical performance is consistent with their different types of formation, since SJ and DPA are defined as volcanic igneous rocks, with aphanitic texture, and SBS as plutonic igneous rock, with phaneritic texture. Although plutonic igneous rocks have satisfactory mechanical resistance due to the relative homogeneity of rock bodies in addition to the mineralogical composition that holds minerals of high hardness, the high granulation of their minerals promotes points of weakness in the rock, increasing the occurrence of micro fractures and consequently decreasing the material mechanical strength (Curtis Neto et al., 2018; Back et al., 2021; Adomaki et al., 2021). This fact justifies the superior mechanical performance of SJ and DPA, since they have

aphanitic texture and/or fine granulation, thus presenting better distributions of mechanical efforts.

The presence of large percentages of alkali feldspar corroborates to the high abrasive loss of SBS, which contains minerals of high hardness (e.g., feldspar: 6 and quartz: 7) with the rocky matrix and show low tenacity due to the granulation. Similarly, the presence of foliation also influences the SBS mechanical performance since it adds horizontal weakness planes that tend to generate a higher percentage of lamellar aggregates in the crushing process and these particles tend to break in the compaction process (Wojahn et al., 2021). In addition to the abrasive loss, there is high loss due to impact and crushing.

Regarding the high percentage of olivine in the SJ rock, it appears that such mineral does not have a dominant influence on the basaltic rock. Although it presents tendencies to alterability, still exhibits excellent results in laboratory tests of mechanical performance and soundness, showing a relatively healthy behavior.

**Table 1.** Mineralogical composition and rock characterization.

	SJ	DPA	SBS
Essential minerals	40% Plagioclase 30% Clinopyroxene 20% Olivine 10% Oxides	35% Feldspar 32% Quartz 25% Pyroxene 8% Opaque	45% K-Feldspar 20% Quartz 20% Biotite 15% Plagioclase
Secondary minerals	Biotite Oxides	Opaque	Mafics Oxides
Carbonate minerals	Absent	Absent	Absent
Deleterious minerals	Oxides	Absent	Mafics Oxides
Structure	Massive	Massive	Foliated
Texture	Aphanitic	Very thin porphyritic inequigranular aphanitic	Inequigranular phaneritic
Rock Type (DNER, 1994a)	Basalt	Rhyodacite	Syenogranite
Rock acidity nature	Basic	Acidic	Acidic
Petrographic thin section slides under polarized light (scale: 100 pixels)			
Specific Gravity (g/cm <sup>3</sup> ) (DNER, 1997a)	2.87	2.5	2.61
Water Absorption (%) (DNER, 1997a)	1.19	2.19	0.69
Sodium sulphate soundness (%) (DNER, 1994b)	5.62 – C 5.70 – F	0.66 – C 5.61 – F	1.72 – C 8.98 – F
“LA” Abrasion (%) (DNER, 1998a)	12.56	10.05	26.39
Impact value (%) (DNER, 1999)	8.44	4.66	18.70
Crushing value (%) (DNER, 1997b)	13.73	13.17	26.38

Where: C: coarse aggregate; F: fine aggregate.

## 2.2 Experimental program

The granulometric curve adopted for the evaluated UGM is in accordance with a highway road standard (DNER, 1998b). The material from the aforementioned rock deposits went through separation, sieving and mixing procedures in order to obtain the specified UGM. A single granulometric curve was used for the three unbound granular materials, which was included within the limits of the most used specifications for the granular base layers of Brazil's southern region by the federal highway agencies (range C) (DNIT, 2006) and state highway agencies (maximum size 3/4") (DAER, 1991). Figure 2 shows the selected particle size distribution.

The samples were subjected to the compaction test to determine the maximum dry density (MDD) and

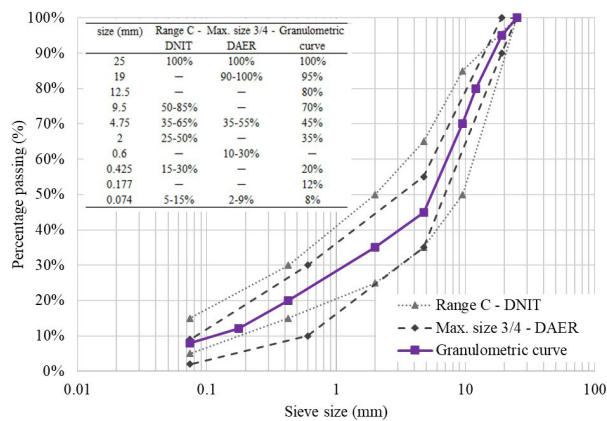


Figure 2. Granulometric curve.

the optimum moisture content (OMC). The compaction process follows the procedures described in the standards of resilient modulus (DNIT, 2018a) and permanent deformation (DNIT, 2018b), similar to the technical procedures adopted by American Association of State Highway and Transportation Officials (AASHTO, 2004), Australia (AGPT, 2006) and the European Union (BSI, 2004). For this, a three-part cylindrical steel mold with dimensions of 200 mm in height and 100 mm in diameter was used. The compaction energy used was equivalent to that of the modified energy. Samples were considered valid for RM and PD tests if the variation was not superior than  $\pm 1\%$  in relation to the MDD and OMC.

The repeated load triaxial equipment used is located in the Department of Transportation from *Universidade Federal de Santa Maria* (UFSM). In the RM test, firstly 1,500 cycles are applied for conditioning the sample; then the test proposes the application of a 100 load cycles for each of 18 pairs of confining stress and deviator stress (DNIT, 2018a). The test was performed in triplicate and with a loading frequency of 1 Hz. Figure 3 presents a sample of UGM compacted in the conditions mentioned above, being positioned in the equipment for a subsequent RLT test.

After the resilient modulus test, the test data were adjusted to mathematical models that were representative of the paving materials mechanical behavior. The mathematical models that can describe the behavior of granular materials regarding resilience, pointed out in the technical literature and cited in this study, are in Table 2. For multiple nonlinear analysis, we used the software Statistica v.10.0.228.2, for linear analysis we used the software Microsoft Office Excel 2013.

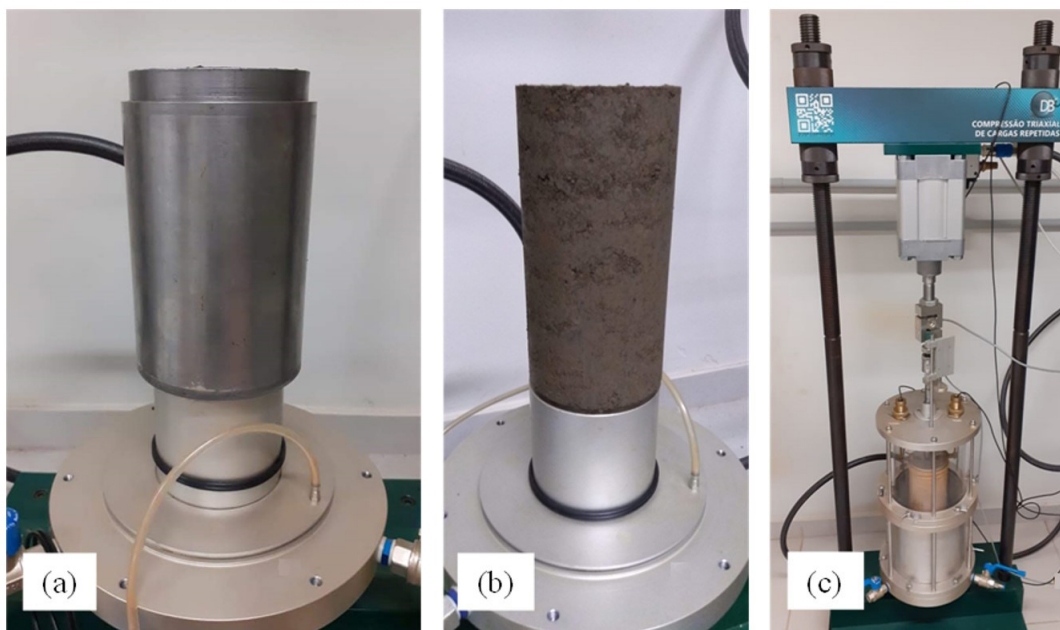


Figure 3. UGM sample being positioned on equipment (a, b) and viewed from the equipment set (c).

In order to evaluate the plasticization to which the granular materials are subjected, the permanent deformation tests were carried out (DNIT, 2018b). Again, the RLT was used to obtain the experimental data. In this test, 100 conditioning cycles are applied for conditioning phase with the 30×30 kPa stresses pair. It is followed by the application of 150,000 charging cycles of each stress pair. For this study, the test protocol was performed according to Lima et al. (2019), with six samples and application of the following single stage stresses (confining versus deviator): 40×40 kPa, 40×120 kPa, 80×80 kPa, 80×240 kPa, 120×240 kPa and 120×360 kPa.

Among the models for predicting permanent deformation of granular materials, the models of Barksdale (1972), Monismith et al. (1975), Uzan (1985) and Tseng & Lytton (1989) stand out. However, for the coherent characterization of tropical materials and their particularities, the model that seems more adequate is the Guimarães' model (Guimarães et al., 2018; Lima et al., 2020), a model used in this research and addressed in Brazilian regulations (Equation 8). The parameters  $\psi_1$ ,  $\psi_2$ ,  $\psi_3$  and  $\psi_4$  were obtained by software Statistica v.10.0.228.2. The parameters of the Guimarães' model are essential to characterize and understand the deformability of soils and unbound granular materials, mainly due de advance of the Brazilian M-E Design Method (MeDiNa).

$$\varepsilon_p (\%) = \psi_1 \left( \frac{\sigma_3}{\rho_a} \right)^{\psi_2} \left( \frac{\sigma_d}{\rho_a} \right)^{\psi_3} N^{\psi_4} \quad (8)$$

Where:  $\varepsilon_p (\%)$  : specific permanent deformation;  $\psi_1$ ,  $\psi_2$ ,  $\psi_3$  and  $\psi_4$ : regression parameters;  $\sigma_3$ : confining stress;  $\sigma_d$ : deviator stress;  $\rho_a$ : atmospheric pressure; N: number of loading cycles.

### 3. Results and analysis

The results are presented in four distinct topics, in the following order: results of sample compaction; resilient modulus, permanent deformation and the relationship between void ratio and deformability.

#### 3.1 Compaction

The results from the compaction tests in this study are shown in Figure 4. SJ basalt granular material reached higher densities, due the high specific gravity of the basalt aggregates. The DPA rhyodacite showed the highest OMC and lowest density among all samples. According to Paiva (2017), this rock presents devitrification of the rock matrix, which is replaced by clay minerals, thus increasing porosity and absorption, justifying the high optimum moisture content.

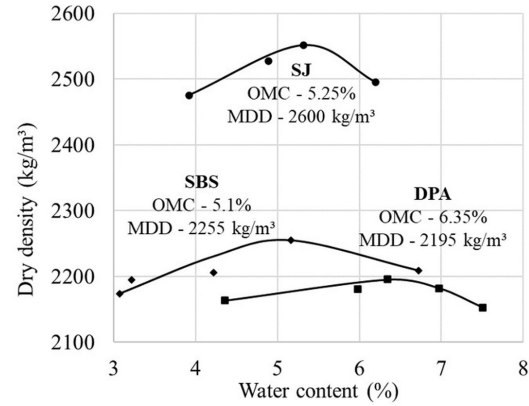


Figure 4. Sample compaction curve.

Table 2. Mathematical models of RM prediction.

Models	Equation
Model k- $\sigma_3$ (Biarez, 1962)	$RM = k_1 \cdot \sigma_3^{k_2}$ (1)
Model k- $\sigma_d$ (Svenson, 1980)	$RM = k_1 \cdot \sigma_d^{k_2}$ (2)
Model k- $\theta$ (Seed et al., 1967)	$RM = k_1 \cdot \theta^{k_2}$ (3)
Compound model (Pezo et al., 1992)	$RM = k_1 \cdot \sigma_3^{k_2} \cdot \sigma_d^{k_3}$ (4)
Universal model (AASHTO, 2004)	$RM = k_1 \cdot \rho_a \left( \frac{\theta}{\rho_a} \right)^{k_2} \cdot \left( \frac{\tau_{oct}}{\rho_a} + 1 \right)^{k_3}$ (5)
Witczak's model (Rada & Witczak, 1981)	$RM = k_1 \cdot \left( \frac{\theta}{\rho_a} \right)^{k_2} \cdot \left( \frac{\sigma_d}{\rho_a} \right)^{k_3}$ (6)
Witczak's and Uzan's model (Witczak & Uzan, 1988)	$RM = k_1 \cdot \rho_a \left( \frac{\theta}{\rho_a} \right)^{k_2} \cdot \left( \frac{\tau_{oct}}{\rho_a} \right)^{k_3}$ (7)

Where:  $RM$ : resilient modulus;  $\sigma_3$ : confining stress;  $\sigma_d$ : deviator stress;  $\theta$ : first stress invariant ( $\theta = \sigma_1 + 2\sigma_3 = \sigma_d + 3\sigma_3$ );  $\tau_{oct}$ : octahedral shear stress;  $\rho_a$ : atmospheric pressure;  $k_1$ ,  $k_2$  and  $k_3$ : regression parameters.

The SBS syenogranite, on the other hand, has the lowest OMC among the mixtures due to its lower absorption, as mentioned in Table 1.

### 3.2 Resilient modulus

In order to evaluate the stiffness properties of the UGMs samples, after the repeated load triaxial tests the laboratory results were analyzed and submitted to mathematical modeling by means of models  $k-\sigma_3$ ,  $k-\sigma_d$ ,  $k-\theta$ , Compound, Universal, Witczak and Witczak and Uzan. The regression parameters are presented in Table 3 with the values of the coefficient of determination ( $R^2$ ) and the value

of the linear resilient modulus, that is, the average of the RM values obtained for each stress pair after performing the mathematical modeling.

The model  $k-\sigma_3$  presents high  $R^2$ , evidencing the strong relationship between the resilient modulus and the confining stress for granular materials; while the model  $k-\sigma_d$ , usually more appropriate to represent soils behavior, presents low  $R^2$ . Based on Table 3, the mathematical models that consider both stresses, confining and deviator, are more representative of the material behavior; in this case are mentioned the models Compound, Universal and Witczak, Witczak and Uzan. The first two of which, for SJ basalt, are exemplified in Figure 5.

**Table 3.** Parameters of mathematical modeling of RM.

		SJ	DPA	SBS
Model $k-\sigma_3$ $RM = k_1 \cdot \sigma_3^{k_2}$	$k_1$	2046	1828	2048
	$k_2$	0.703	0.772	0.768
	$R^2$	0.930	0.946	0.959
	RM avg (MPa)	304	227	257
Model $k-\sigma_d$ $RM = k_1 \cdot \sigma_d^{k_2}$	$k_1$	916.96	742.88	826.64
	$k_2$	0.533	0.578	0.571
	$R^2$	0.793	0.784	0.781
	RM avg (MPa)	300	223	252
Model $k-\theta$ $RM = k_1 \cdot \theta^2$	$k_1$	656.4	520.9	585.8
	$k_2$	0.690	0.755	0.784
	$R^2$	0.955	0.960	0.968
	RM avg (MPa)	305	228	249
Compound model $RM = k_1 \cdot \sigma_3^{k_2} \cdot \sigma_d^{k_3}$	$k_1$	2256.46	1983.87	1896.11
	$k_2$	0.589	0.665	0.612
	$k_3$	0.196	0.18	0.164
	$R^2$	0.977	0.981	0.982
	RM avg (MPa)	306	229	258
Universal model $RM = k_1 \cdot \rho_a \left( \frac{\theta}{\rho_a} \right)^{k_2} \cdot \left( \frac{\tau_{oct}}{\rho_a} + 1 \right)^{k_3}$	$k_1$	1206.47	829.12	1029.97
	$k_2$	0.863	0.985	0.915
	$k_3$	-0.213	-0.358	-0.355
	$R^2$	0.973	0.977	0.980
	RM avg (MPa)	306	228	258
Witczak's model $RM = k_1 \cdot \left( \frac{\theta}{\rho_a} \right)^{k_2} \cdot \left( \frac{\sigma_d}{\rho_a} \right)^{k_3}$	$k_1$	103.18	67.18	84.43
	$k_2$	0.928	1.045	0.962
	$k_3$	-0.145	-0.202	-0.188
	$R^2$	0.977	0.979	0.982
	RM avg (MPa)	306	227	258
Witczak's and Uzan's model $RM = k_1 \cdot \rho_a \left( \frac{\theta}{\rho_a} \right)^{k_2} \cdot \left( \frac{\tau_{oct}}{\rho_a} \right)^{k_3}$	$k_1$	925.11	576.79	732.61
	$k_2$	0.928	1.045	0.962
	$k_3$	-0.141	-0.203	-0.188
	$R^2$	0.977	0.979	0.982
	RM avg (MPa)	306	227	258

For the Compound model, coefficient  $k_2$  referring to the confining stress action has higher impact on the RM value to the detriment of coefficient  $k_3$  related to the deviator stress. However, the fact that the coefficient  $k_3$  has a positive value indicates that, by increasing the deviator stress, an increase in the resilient modulus occurs. The Compound model is the most discussed in this study since it is currently used in the Brazilian M-E Design Method (MeDiNa) for characterization related to the stiffness of subgrade soils and granular materials (Guimarães & Motta, 2016; Freitas et al., 2020; Lima et al., 2020; Sagrilo, 2020; Pascoal et al., 2021; Zago et al., 2021; Pascoal et al., 2023).

The analysis of the Universal model indicates that the increase of the first stress invariant collaborate to the RM of the material, by the positive value of  $k_2$ . On the other hand, the coefficient  $k_3$  presented a negative value due to the increase in the octahedral shear stress, causing a lower RM value. This is similar to the Witczak's and Uzan's model, in which coefficients  $k_2$  and  $k_3$  are related to the same stresses as the Universal model. The model by Witczak also demonstrate that the increase of first stress invariant reflects in a higher

RM, due to the positive value of  $k_2$  for all materials; although the increase of the deviator stress does not strongly affect the RM, due to the negative and low value of  $k_3$ .

### 3.3 Permanent deformation

In order to understand the behavior of the granular material subjected to damage by permanent deformation, the UGM of different lithologies were submitted to the RLT test of long duration. Subsequently, the shakedown analysis was carried out according to Werkmeister (2003), the Guimarães' model was implemented to the mixtures and loss or gain of stiffness of the samples was verified after the stress history of the PD test.

Figures 6, 7 and 8 show the graphs representing the permanent deformation tests of UGM SJ, DPA and SBS, respectively. The graphs at the left (a) show the accumulated PD versus number of cycles, so the increase rate of the curve gives evidence of stabilization or not of these deformations; the right graph line shows the behavior of the permanent deformation increase rate over the accumulation of deformations.

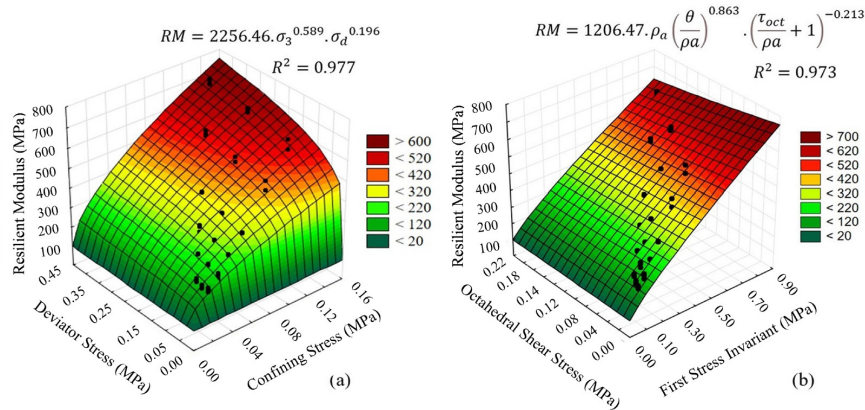


Figure 5. Examples of the statistical fitting – Compound (a) and Universal (b) Models for SJ.

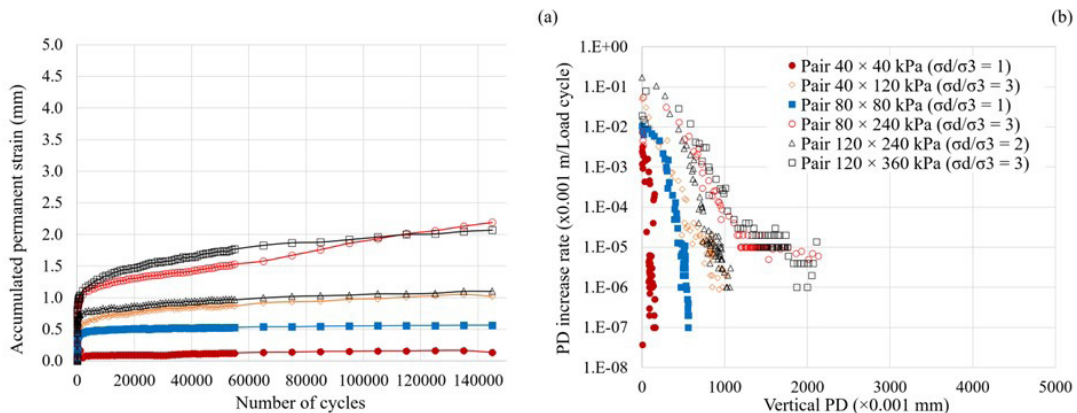


Figure 6. Permanent deformation test results – SJ: accumulated PD (a) and PD increase rate (b).

For SJ basalt the highest permanent deformations recorded were observed in tests whose stress pairs are 120×360 kPa and 80×240 kPa, confining versus deviator, respectively, reaching values close to 2.3 mm at the end of the tests (Figure 6a). The pair 120×240 kPa presented considerably smaller deformations than the pairs 120×360 kPa and 80×240 kPa. The smallest deformations were found in the 40×40 kPa e 80×80 kPa tests. This behavior indicates that the permanent deformations magnitude is related to the ratio among  $\sigma_d / \sigma_3$  in a directly proportional relation. Similar results were pointed out by Lekarp et al. (2000), Lima et al. (2017) and Delongui et al. (2018).

Observing the increase rate graph in PD by the cumulative vertical deformation of the SJ it can be seen that only tests whose stress ratio  $\sigma_d / \sigma_3$  is equal to one entered shakedown (i.e., type A behavior) according to the parameters of Dawson & Wellner (1999) and Werkmeister (2003) with the permanent deformation increase rate in  $10^{-7} \times 10^{-3}$  meters per load application cycle in 150000 cycles. Those tests are presented in the Figure 6b with filled markers. The other pairs presented creep shakedown, i.e., behavior B. Projecting the PD values

with the Guimarães' model, the pair 40×120 kPa would reach the rate of  $10^{-7} \times 10^{-3}$  meters per load application cycle in 155000 cycles, while the same would happen to the pair 120×240 kPa at 185000 cycles.

For the DPA rhyodacite the deformation results were similar to that observed with basalt, in relation to the pairs that deformed more or less, as well as the value of higher accumulated deformation, close to 2.5 mm (Figure 7a). The 40×40 kPa pair reached the accommodation – behavior A, as it possible to see in Figure 7b; the same happened to the pair 80×80 kPa by the projection of the Guimarães' model for this material, reaching  $10^{-7} \times 10^{-3}$  meters per load application cycle. The other pairs present behavior B.

Syenogranite, an aggregate with a different texture from the others, presented considerably higher plastic deformability than the other analyzed materials. The highest deformation observed was approximately 5 mm, although the densities obtained in the compaction test were close to that for the rhyodacite (Figure 8a). This behavior seems to be related to this rock's inferior mechanical performance in relation to the others with respect to the laboratory tests of mechanical characterization, as previously shown in Table 1.

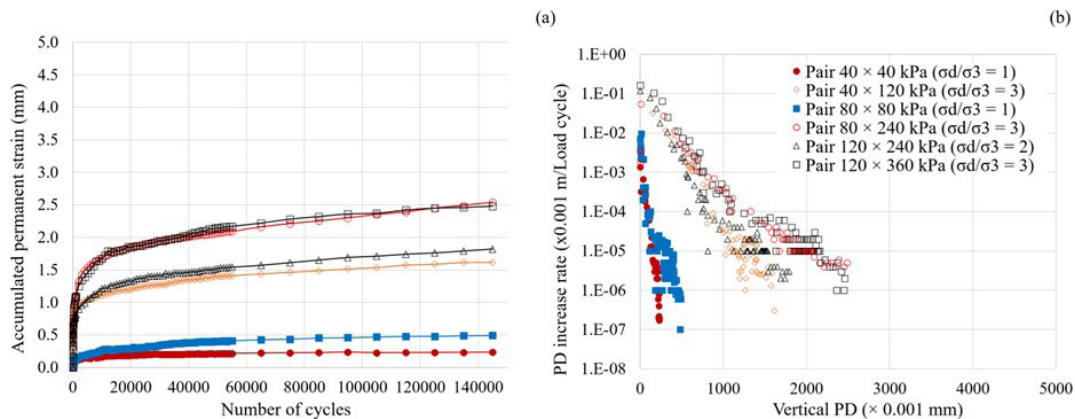


Figure 7. Permanent deformation test results – DPA: accumulated PD (a) and PD increase rate (b).

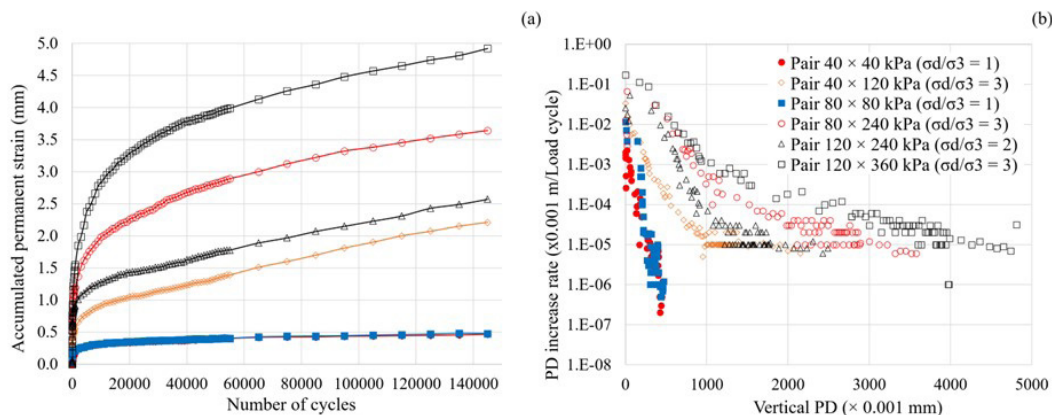


Figure 8. Permanent deformation test results – SBS: accumulated PD (a) and PD increase rate (b).

The stress pairs that showed a tendency to shakedown with the highest number of cycles are the pairs with  $\sigma_d / \sigma_3$  is equal to one - 40×40 kPa and 80×80 kPa (Figure 8b). Other pairs present type B behavior.

The materials were, by multiple nonlinear regression analysis, mathematically characterized as to their PD by the Guimarães' model. The parameters obtained for the specific permanent deformation are in Table 4. From the parameters and the coefficient of determination, it is evident that the Guimarães' model is representative of the deformability of the materials under study; also noticeable is the strong impact of the deviator stress in the PD, represented by the high values of  $\psi_3$ , a trend already observed in Figures 6, 7 and 8 by relations  $\sigma_d / \sigma_3$ .

The stiffness gain of samples submitted to stress history was evaluated by the resilient modulus test after the permanent deformation test. It was possible to compare the average RM value after the test for each stress pair and the value obtained for the conventional RM test. The average RM for Compound Model after each PD test is shown in Figure 9 in a bar format, while the horizontal line represents the conventional RM test. In addition, in the center of each bar, it is shown the shakedown behavior of each sample, in this case, A or B.

It is possible to infer that there is a relationship among the lithological type, resilient behavior and shakedown. For basalt, after the PD test, all samples show a relative loss of stiffness in relation to the conventional RM, a result similar to that obtained by Guimarães (2009) for other basaltic material; it is also clear that this loss is not proportionally evidenced among all pairs. For those whose behavior towards shakedown pointed to behavior B, the loss was more significant. For rhyodacite, only the pairs that demonstrated accommodation of the particles had the stiffness increase of the samples with the history of stresses; the other pairs lost stiffness, as expressive as the higher the deformations undergone. Finally, for the syenogranite all samples gained stiffness after the long-term PD test, with the exception of the last pair. Close results were obtained by Lima et al. (2017) and Norback (2018) for UGM of similar origin. It is also noticed that the pairs that had behavior A towards the shakedown had an increase in RM which was more significant than the others. For all the materials, according to Figure 9, as the deviator stress increases for the same confining stress, the resilient modulus of the material decreases, in accordance to

shakedown theory. A deeper investigation must be conducted in order to verify any relationship between this decrease and the type of aggregate.

### 3.4 Void ratio and deformability

Based on physical indexes and compaction parameters, it was observed a relation between the samples void ratio and its RM. This behavior seems to be dependent on the lithological origin of the UGM. Figure 10 exhibits the results of average RM for Compound model and void ratio; the filled markers represent the RM after PD and the not filled markers denote the conventional RM test.

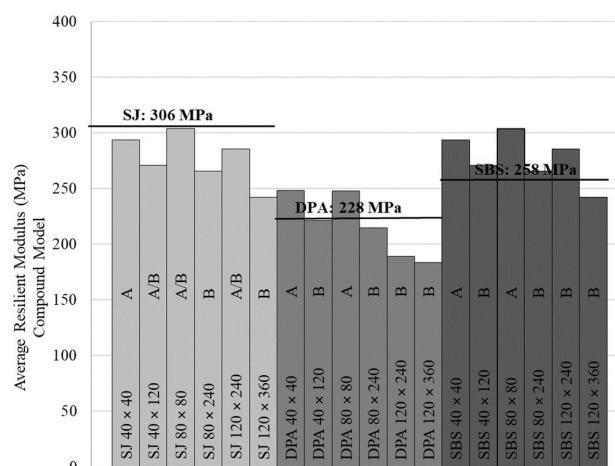


Figure 9. Relationship between conventional RM and after PD – SJ, DPA and SBS.

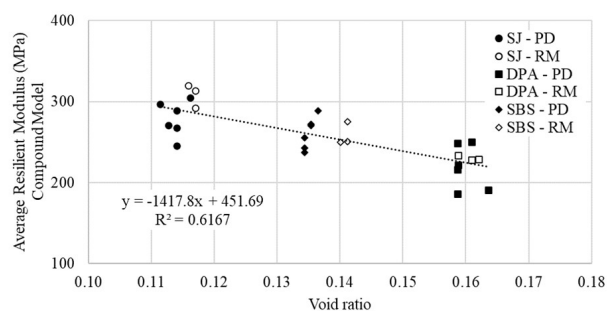


Figure 10. Void ratio vs average RM for SJ, DPA, SBS granular materials.

Table 4. Parameters of permanent deformation from the Guimarães' model (Guimarães, 2009).

		SJ	DPA	SBS
Guimarães' model (Guimarães, 2009)	$\psi_1$	0.048	0.040	0.019
	$\psi_2$	-0.622	-0.892	-0.908
	$\psi_3$	1.188	1.311	1.816
	$\psi_4$	0.138	0.169	0.226
	$R^2$	0.938	0.967	0.989

Basalt SJ presented the highest modulus, followed by SBS syenogranite and DPA rhyodacite, opposed to the void ratio achieved in the compaction. Based on this work, materials with different properties - such as abrasion, shape, texture and crushing process, even with the same particle size distribution, followed a trendline that suggest that void ratio may be a key parameter to predict RM.

Currently, we are researching the relation between stress state and physical indexes and the densification, gain of stiffness and loss of void volume during the PD test. This research topic is still in progress and is not fully developed, so we limited the contribution in the present manuscript for this initial analysis.

#### 4. Final considerations

This research aimed, by means of laboratory tests and mathematical modeling, to understand the deformability, especially resilient modulus and permanent deformation, of unbound granular materials. For this purpose, the granulometric curve was kept constant with the basalt, rhyodacite and syenogranite, materials representative of the Brazilian state of Rio Grande do Sul.

The stiffness of the materials, expressed by the resilient modulus, was tested and mathematically represented by models  $k-\sigma_3$ ,  $k-\sigma_d$ ,  $k-\theta$ , Compound, Universal, Witczak and Witczak and Uzan. The models that demonstrated the best fitting were those that consider the action of the confining and deviator stresses. In accordance to the literature, granular materials are mostly confining stress dependent; which was stated in this research as well.

The performance of the three UGMs regarding to RM and PD were different. For damage by permanent deformation, the trend found for the RM was not maintained. Syenogranite, for example, presented the worst behavior in view of permanent deformation, even though showed an intermediate RM. This effect may be related to the greater granulation of the minerals of the SBS rock in addition to the foliated structure, which starts to show poor mechanical behavior (see results for LA abrasion, impact value and crushing value). These mechanical characteristics result in the breaking of the particles promoted by the zones of weaknesses among the minerals, promoting a thinner granulometric curve, liable to high permanent deformations.

The Guimarães' model proved to be adequate to represent the PD of the materials under study, showing a high coefficient of determination. Some pairs seemed to show accommodation after 150000 cycles, and the model made it possible to predict the number of cycles needed. Furthermore, this study described a relationship between the conventional RM and after the PD test, lithological origin and shakedown.

Also, this study showed a relevant relation between the void ratio of the compacted UGM and its resilient modulus. The void ratio is affected by aggregate shape, texture, rock crushing processes and compaction parameters; this could be, with deeper investigation, a key parameter to predict RM.

#### Acknowledgements

The authors would like to thank ANP/Petrobras, Conselho Nacional de Desenvolvimento Científico e Tecnológico (CNPq), Coordenação de Aperfeiçoamento de Pessoal de Nível Superior (CAPES) for their financial support and the reviewers of Soils and Rocks for their valuable contributions.

#### Declaration of interest

The authors have no conflicts of interest to declare. All co-authors have observed and affirmed the contents of the paper and there is no financial interest to report.

#### Authors' contributions

Amanda Vielmo Sagrilo: conceptualization, data curation, visualization, methodology and experimental procedures, writing – original draft, review & editing. Paula Taiane Pascoal: validation, methodology and experimental procedures, writing – review & editing. Magno Baroni: supervision, validation, writing – review & editing. Ana Helena Back: validation, methodology and experimental procedures, writing – review & editing. Rinaldo José Barbosa Pinheiro: supervision, validation, writing – review. Luciano Pivoto Specht: supervision, funding acquisition, project administration, writing – review. Antônio Carlos Rodrigues Guimarães: supervision, validation, writing – review.

#### Data availability

The datasets produced and analyzed in the course of the present study are available from the corresponding author upon reasonable request.

#### List of symbols

$k_1, k_2, k_3$	resilient parameters experimentally determined
<i>DPA</i>	granular material from Della Pasqua quarry
<i>N</i>	number of loading cycles
<i>PD</i>	permanent deformation
$R^2$	coefficient of determination
<i>RLT</i>	repeated load triaxial
<i>RM</i>	resilient modulus
<i>SBS</i>	granular material from SBS Engenharia quarry
<i>SJ</i>	granular material from São Juvenal quarry
<i>UFMS</i>	Universidade Federal de Santa Maria
<i>UGM</i>	unbound granular material
<i>UTM</i>	Universal Transverse Mercator coordinate system
$\varepsilon_p$	specific permanent deformation
$\theta$	principal stress
$\rho_a$	atmospheric pressure

$\sigma_3$	confining stress
$\sigma_d$	deviator stress
$\sigma_d / \sigma_3$	stress ratio
$\tau_{oct}$	octahedral stress
$\Psi_1, \Psi_2, \Psi_3, \Psi_4$	permanent deformation parameters experimentally determined

## References

- AASHTO NCHRP 1-37A. (2004). *Guide for mechanistic-empirical design of new and rehabilitated pavement structure - Final report*. Transportation Research Board, Washington, DC.
- Adomaki, S., Engelsen, C.J., Thorstensen, R.J., & Barbieri, D.M. (2021). Review of the relationship between aggregates geology and Los Angeles and micro-Deval tests. *Bulletin of Engineering Geology and the Environment*, 80, 1963-1980. <http://dx.doi.org/10.1007/s10064-020-02097-y>.
- AGPT T053. (2006). *Determination of permanent deformation and resilient modulus characteristics of unbound granular materials under drained conditions*. Austroads, Sydney.
- Alnedawi, A., Klafe, B., Ullah, S., & Kerr, W. (2021). Investigation of non-standard unbound granular materials under cyclic loads: experimental and regression analyses. *The International Journal of Pavement Engineering*, 23(9), 2998-3010. <http://dx.doi.org/10.1080/10298436.2021.1877291>.
- Alnedawi, A., Nepal, K.P., & Al-Ameri, R. (2019a). New shakedown criterion and permanent deformation properties of unbound granular materials. *Journal of Modern Transportation*, 27(2), 108-119. <http://dx.doi.org/10.1007/s40534-019-0185-2>.
- Alnedawi, A., Nepal, K.P., & Al-Ameri, R. (2019b). Permanent deformation prediction model of unbound granular materials for flexible pavement design. *Transportation Infrastructure Geotechnology*, 6, 39-55. <http://dx.doi.org/10.1007/s40515-018-00068-1>.
- Ba, M., Tinjum, J.M., & Fall, M. (2015). Prediction of permanent deformation model parameters of unbound base course aggregates under repeated loading. *Road Materials and Pavement Design*, 16(4), 854-869. <http://dx.doi.org/10.1080/14680629.2015.1063534>.
- Back, A.H., Ceccato, H.D., Pinheiro, R.J.B., Nummer, A.V., & Sagrilo, A.V. (2021). Avaliação do comportamento característico de rochas vulcânicas da formação Serra Geral e sua implementação em obras rodoviárias. *Geociências*, 40, 1125-1136. <http://dx.doi.org/10.5016/geociencias.v40i04.15845>.
- Barksdale, R.D. (1972). Laboratory evaluation of rutting in base course materials. In *Proceedings of the 3rd International Conference on the Structural Design of Asphalt Pavements* (pp. 161-174). Ann Arbor: University of Michigan.
- Biarez, J. (1962). *Contribution a l'étude des propriétés mécaniques des sols et des matériaux pulvérants* [Doctoral thesis]. Faculté des Sciences Grenoble.
- BSI EN 13286-7. (2004). *Unbound and hydraulically bound mixtures - part 7: cyclic load triaxial test for unbound mixtures*. British Standards Institution, London.
- Carvalho, J.C., Rezende, L.R., Cardoso, F.B.F., Lucena, L.C.F.L., Guimarães, R.C., & Valencia, Y.G. (2015). Tropical soils for highway construction: peculiarities and considerations. *Transportation Geotechnics*, 5, 3-19. <http://dx.doi.org/10.1016/j.trgeo.2015.10.004>.
- Cerni, G., Cardone, F., Virgili, A., & Camilli, S. (2012). Characterisation of permanent deformation behavior of unbound granular materials under repeated triaxial loading. *Construction & Building Materials*, 28, 79-87. <http://dx.doi.org/10.1016/j.conbuildmat.2011.07.066>.
- Collins, I.F., & Boulbibane, M. (2000). Geomechanical analysis of unbound pavements based on shakedown theory. *Journal of Geotechnical and Geoenvironmental Engineering*, 126(1), 50-59. [http://dx.doi.org/10.1061/\(ASCE\)1090-0241\(2000\)126:1\(50\)](http://dx.doi.org/10.1061/(ASCE)1090-0241(2000)126:1(50)).
- Curtis Neto, J.A., Ribeiro, R.P., Watashi, D.B., Paraguassu, A.B., Santos, R.S., & Xavier, G.C. (August-September, 28-01, 2018). Comparação estatística entre ensaios mecânicos de agregados pétreos. In *8º Simpósio Brasileiro de Mecânica das Rochas*, Salvador, Brazil (in Portuguese).
- DAER ES-P 08/91. (1991). *Base granular*. DAER – Departamento Autônomo de Estradas de Rodagem, Porto Alegre, RS (in Portuguese).
- Dawson, A.R., & Wellner, F. (1999). *Plastic behavior of granular materials. Report ARC project 933. Reference PRG 99014*. University of Nottingham.
- Delongui, L., Matuella, M., Núñez, W.P., Fedrigo, W., Silva Filho, L.C.P., & Ceratti, J.A.P. (2018). Construction and demolition waste parameters for rational pavement design. *Construction & Building Materials*, 168, 105-112. <http://dx.doi.org/10.1016/j.conbuildmat.2018.02.086>.
- DNER 006. (1994a). *Materiais rochosos usados em rodovias – análise petrográfica – instrução de ensaio DNER 006*. DNER - Departamento Nacional de Infraestrutura de Transportes, Rio de Janeiro, RJ (in Portuguese).
- DNER 195. (1997a). *Agregado – determinação da absorção e da densidade do agregado graúdo – método de ensaio DNER 195*. DNER - Departamento Nacional de Infraestrutura de Transportes, Rio de Janeiro, RJ (in Portuguese).
- DNER 197. (1997b). *Agregado graúdo – determinação da resistência do esmagamento – método de ensaio DNER 197*. DNER - Departamento Nacional de Infraestrutura de Transportes, Rio de Janeiro, RJ (in Portuguese).
- DNER 35. (1998a). *Agregado graúdo – ensaio de abrasão “Los Angeles” – método de ensaio DNER 35*. DNER - Departamento Nacional de Infraestrutura de Transportes, Rio de Janeiro, RJ (in Portuguese).
- DNER 399. (1999). *Agregados - determinação da perda ao choque no aparelho Treton – método de ensaio DNER 399*. DNER - Departamento Nacional de Infraestrutura de Transportes, Rio de Janeiro, RJ (in Portuguese).

- DNER 83. (1998b). *Agregado – análise granulométrica - método de ensaio DNER 83*. DNER - Departamento Nacional de Infraestrutura de Transportes, Rio de Janeiro, RJ (in Portuguese).
- DNER 89. (1994b). *Avaliação da durabilidade pelo emprego de soluções de sulfato de sódio ou de magnésio – método de ensaio DNER 89*. DNER - Departamento Nacional de Infraestrutura de Transportes, Rio de Janeiro, RJ (in Portuguese).
- DNIT 134. (2018a). *Pavimentação – solos – determinação do módulo de resiliência – método de ensaio DNIT 134*. DNIT - Departamento Nacional de Infraestrutura de Transportes, Rio de Janeiro, RJ (in Portuguese).
- DNIT 179. (2018b). *Pavimentação - solos - determinação da deformação permanente – instrução de ensaio DNIT 179*. DNIT - Departamento Nacional de Infraestrutura de Transportes, Rio de Janeiro, RJ (in Portuguese).
- DNIT. (2006). *Manual de pavimentação*. DNIT - Departamento Nacional de Infraestrutura de Transportes, Rio de Janeiro, RJ (in Portuguese).
- Erlingsson, S., Rahman, S., & Salour, F. (2017). Characteristics of unbound granular materials and subgrades based on multi stage RLT testing. *Transportation Geotechnics*, 13, 28-42. <http://dx.doi.org/10.1016/j.trgeo.2017.08.009>.
- Freitas, J.B., Rezende, L.R., & Gitirana Junior, G.F.N. (2020). Prediction of the resilient modulus of two tropical subgrade soils considering unsaturated conditions. *Engineering Geology*, 270, 105580. <http://dx.doi.org/10.1016/j.enggeo.2020.105580>.
- Gu, F., Zhang, Y., Luo, X., Sahin, H., & Lytton, R.L. (2017). Characterization and prediction of permanent deformation properties of unbound granular materials for Pavement ME Design. *Construction & Building Materials*, 155, 584-592. <http://dx.doi.org/10.1016/j.conbuildmat.2017.08.116>.
- Guimarães, A.C.R. (2009). *Um método mecanístico - empírico para a previsão da deformação permanente em solos tropicais constituintes de pavimentos* [Doctoral thesis, Federal University of Rio de Janeiro]. Federal University of Rio de Janeiro's repository (in Portuguese). Retrieved in May 18, 2023, from <http://www.coc.ufjf.br/pt/teses-de-doutorado/153-2009/1199-antonio-carlos-rodrigues-guimaraes>
- Guimarães, A.C.R., & Motta, L.M.G. (2016). Mechanical behavior of basaltic rocks from Serra Geral Formation used as road material in Santa Catarina State, Brazil. *Soils and Rocks*, 39(2), 203-210. <http://dx.doi.org/10.28927/SR.392203>.
- Guimarães, A.C.R., Motta, L.M.G., & Castro, C.D. (2018). Permanent deformation parameters of fine - grained tropical soils. *Road Materials and Pavement Design*, 20(7), 1664-1681. <http://dx.doi.org/10.1080/14680629.2018.1473283>.
- Huang, Y.H. (2004). *Pavement analysis and design*. Editora Prentice Hall.
- Lekarp, F., & Isacsson, U. (2001). The effects of grading scale on repeated load triaxial test results. *The International Journal of Pavement Engineering*, 2(2), 85-101. <http://dx.doi.org/10.1080/10298430108901719>.
- Lekarp, F., Isacsson, U., & Dawson, A. (2000). State of the art II: permanent strain response of unbound aggregates. *Journal of Transportation Engineering*, 126(1), 76-83. [http://dx.doi.org/10.1061/\(ASCE\)0733-947X\(2000\)126:1\(76\)](http://dx.doi.org/10.1061/(ASCE)0733-947X(2000)126:1(76)).
- Lima, C.D.A., Motta, L.M.G., & Aragão, F.T.S. (November 10-14, 2019). Análise das tensões aplicadas nos ensaios de deformação permanente de solos e britas para o dimensionamento mecanístico-empírico de pavimentos. In Associação Nacional de Pesquisa e Ensino em Transportes (Org.), *33º Congresso de Pesquisa e Ensino em Transportes da ANPET* (pp. 1222-1233). Rio de Janeiro: ANPET (in Portuguese).
- Lima, C.D.A., Motta, L.M.G., & Guimarães, A.C.R. (2017). Estudo da deformação permanente de britas granito-gnaiss para uso em base e sub-base de pavimentos. *Revista Transportes*, 25, 41-52. <http://dx.doi.org/10.14295/transportes.v25i2.1262>.
- Lima, C.D.A., Motta, L.M.G., Aragão, F.T.S., & Guimarães, A.C.R. (2020). Mechanical characterization of fine-grained lateritic soils for mechanistic-empirical flexible pavement design. *Journal of Testing and Evaluation*, 48(1), 1-17. <http://dx.doi.org/10.1520/JTE20180890>.
- Medina, J., & Motta, L.M.G. (2015). *Mecânica dos pavimentos*. Editora Interciência (in Portuguese).
- Monismith, C.L., Ogawa, N., & Freeme, C.R. (January 13-17, 1975). Permanent deformation characteristics of subgrade soils due to repeated loading. In *54º Annual Meeting of TRB*, Washington, United States of America.
- Nazzal, M.D., Mohammad, L.N., & Austin, A. (2020). Evaluating laboratory tests for use in specifications for unbound base course materials. *Journal of Materials in Civil Engineering*, 32(4), 1-8. [http://dx.doi.org/10.1061/\(ASCE\)MT.1943-5533.0003042](http://dx.doi.org/10.1061/(ASCE)MT.1943-5533.0003042).
- Nogami, J.S., & Villibor, D.F. (1991). Use of lateritic fine-grained soils in road pavement base courses. *Geotechnical and Geological Engineering*, 9, 167-182. <http://dx.doi.org/10.1007/BF00881739>.
- Norback, C. (2018). *Caracterização do módulo de resiliência e da deformação permanente de três solos e misturas solo-brita* [Master's dissertation, Federal University of Rio de Janeiro]. Federal University of Rio de Janeiro's repository (in Portuguese). Retrieved in May 18, 2023, from <https://pantheon.ufjf.br/handle/11422/13425>
- Paiva, P.S. (2017). *Caracterização e avaliação das propriedades geomecânicas para uso em pavimentação de agregados de rochas vulcânicas da porção central do Rio Grande do Sul* [Master's dissertation, Federal University of Santa Maria]. Federal University of Santa Maria's repository (in Portuguese). Retrieved in May 18, 2023, from <https://repositorio.ufsm.br/handle/1/14728>

- Pascoal, P.T., Sagrilo, A.V., Baroni, M., Specht, L.P., & Pereira, D.S. (2021). Evaluation of the influence of compaction energy on the resilient behavior of lateritic soil in the field and laboratory. *Soils and Rocks*, 44(4), e2021071321. <http://dx.doi.org/10.28927/SR.2021.071321>.
- Pascoal, P.T., Sagrilo, A.V., Baroni, M., Specht, L.P., & Pereira, D.S. (2023). Lateritic soil deformability regarding the variation of compaction energy in the construction of pavement subgrade. *Soils and Rocks*, 46(3), e2023009922. <https://doi.org/10.28927/SR.2023.009922>.
- Pezo, R.F., Carlos, G., Hudson, W.R., & Stokoe II, K.H. (1992). *Development of reliable resilient modulus test for subgrade and non-granular subbase materials for use in routine pavement design*. Retrieved in May 18, 2023, from <https://trid.trb.org/view/369153>
- Rada, G., & Witzak, M.W. (1981). Comprehensive evaluation of laboratory resilient moduli results for granular materials. *Transportation Research Record: Journal of the Transportation Research Board*, (810), 23-33. Retrieved in May 18, 2023, from <http://onlinepubs.trb.org/Onlinepubs/trr/1981/810/810-004.pdf>
- Sagrilo, A.V. (2020). *Estudo de deformabilidade e empacotamento de britas com diferentes origens litológicas do estado do Rio Grande do Sul* [Master's dissertation, Federal University of Santa Maria]. Federal University of Santa Maria's repository (in Portuguese). Retrieved in May 18, 2023, from <https://repositorio.ufsm.br/handle/1/22211>
- Seed, H.B., Mitry, F. G., Monismith, C. L., Chan, C. K. (1967). *Prediction of flexible pavement deflections from laboratory repeated load tests*. National Cooperative Highway Research Program. Report No. 35.
- Soliman, H., & Shalaby, A. (2015). Permanent deformation behavior of unbound granular base materials with varying moisture and fines content. *Transportation Geotechnics*, 37(4), 1-12. <http://dx.doi.org/10.1016/j.trgeo.2015.06.001>.
- Song, Y., & Ooi, P.S.K. (2010). Interpretation of shakedown limit from multistage permanent deformation test. *Transportation Research Record: Journal of the Transportation Research Board*, (2167), 72-82. <http://dx.doi.org/10.3141/2167-08>.
- Svenson, M. (1980). *Ensaio triaxiais dinâmicos de solos argilosos* [Master's dissertation, Federal University of Rio de Janeiro]. Federal University of Rio de Janeiro's repository (in Portuguese). Retrieved in May 18, 2023, from <https://pantheon.ufjf.br/bitstream/11422/3001/1/152894.pdf>
- Tseng, K.H., & Lytton, R.L. (1989). *Prediction of permanent deformation in flexible pavement materials. Implication of aggregates in the design, construction and performance of flexible pavements* (pp. 154-172). American Society for Testing and Materials.
- Uzan, J. (1985). Characterization of granular material. *Transportation Research Record*, 1022, 52-59. Retrieved in May 18, 2023, from <https://onlinepubs.trb.org/Onlinepubs/trr/1985/1022/1022-007.pdf>
- Wang, J., & Yu, H.S. (2013). Shakedown analysis for design of flexible pavements under moving loads. *Road Materials and Pavement Design*, 14(3), 703-722. <http://dx.doi.org/10.1080/14680629.2013.814318>.
- Werkmeister, S. (2003). *Permanent deformation behavior under granular materials in pavement constructions* [Doctoral thesis]. Dresden University of Technology.
- Werkmeister, S. (June 6-8, 2006). Shakedown analysis of unbound granular materials using accelerated pavement test results from New Zealand's CAPTIF facility. In B. Huang, R. Meier, J. Prozzi & E. Tutumluer (Eds.), *Pavements Mechanics and Performance: Proceedings of Sessions of GeoShanghai* (pp. 220-228). Reston, United States of America: ASCE. [https://doi.org/10.1061/40866\(198\)28](https://doi.org/10.1061/40866(198)28).
- Werkmeister, S., Dawson, A.R., & Wellner, F. (2001). Permanent deformation behavior of granular materials and the shakedown concept. *Transportation Research Record: Journal of the Transportation Research Board*, (1757), 75-81. <http://dx.doi.org/10.3141/1757-09>.
- Witzak, M.W., & Uzan, J. (1988). *The universal airport pavement design system. Report I of V: granular material characterization*. University of Maryland.
- Wojahn, R.E., Clemente, I.M., Back, A.H., Nummer, A.V., & Pinheiro, R.J.B. (2021). Avaliação das propriedades tecnológicas de agregados de composição granítica oriundos de duas jazidas do estado do Rio Grande do Sul. *Anuário do Instituto de Geociências*, 44(36308), 1-12. [http://dx.doi.org/10.11137/1982-3908\\_2021\\_44\\_36308](http://dx.doi.org/10.11137/1982-3908_2021_44_36308).
- Xiao, Y., Tutumluer, E., & Mishra, D. (2019). Performance evaluations of unbound aggregate permanent deformation models for various aggregate physical properties. *Transportation Research Record: Journal of the Transportation Research Board*, 2525(1), 20-30. <http://dx.doi.org/10.3141/2525-03>.
- Zago, J.P., Pinheiro, R.J.B., Baroni, M., Specht, L.P., Delongui, L., & Sagrilo, A.V. (2021). Study of the permanent deformation of three soils employed in highway subgrades in the municipality of Santa Maria-RS, Brazil. *International Journal of Pavement Research and Technology*, 14, 729-739. <http://dx.doi.org/10.1007/s42947-020-0129-6>.